

# The Rotational Excitation Temperature of the $\lambda 6614$ Diffuse Interstellar Band Carrier

J. Cami<sup>1</sup>, F. Salama<sup>1</sup>, J. Jiménez-Vicente<sup>2</sup>, G.A. Galazutdinov<sup>3,4</sup> and J. Krelowski<sup>5</sup>

jcam@mail.arc.nasa.gov

fsalama@mail.arc.nasa.gov

jjimenez@ugr.es

gala@boao.re.kr

Jacek.Krelowski@astri.uni.torun.pl

Received \_\_\_\_\_; accepted \_\_\_\_\_

---

<sup>1</sup>NASA Ames Research Center, MS 245-6, Moffett Field, CA 94035, USA

<sup>2</sup>Depto. Física Teórica y del Cosmos, Fac. de Ciencias, Univ. de Granada, Av. Fuentenueva s/n, 18071 Granada, Spain

<sup>3</sup>Korea Astronomy Observatory, Optical Astronomy Division, 61-1, Whaam-Dong, Yuseong-Gu, Daejeon 305-348, Korea

<sup>4</sup>Special Astrophysical Observatory, Nizhnij Arkhyz 369167, Russia

<sup>5</sup>Center for Astronomy, Nicolaus Copernicus University, Gagarina 11, 87-100 Torún, Poland

## ABSTRACT

Analysis of high spectral resolution observations of the  $\lambda 6614$  diffuse interstellar band (DIB) line profile show systematic variations in the positions of the peaks in the substructure of the profile. These variations – shown here for the first time – can be understood most naturally in the framework of rotational contours of large molecules, where the variations are caused by changes in the rotational excitation temperature. We show that the rotational excitation temperature for the DIB carrier is likely significantly lower than the gas kinetic temperature – indicating that for this particular DIB carrier angular momentum buildup is not very efficient.

*Subject headings:* ISM: lines and bands, ISM: molecules

## 1. Introduction

The diffuse interstellar bands (DIBs) are over 300 interstellar absorption bands commonly observed toward reddened stars from the UV to the near-IR, and whose carrier molecules are still unidentified (Herbig 1995; Krelowski 2003). The identification of the carriers of these bands remains an important problem in astronomy to date and the current consensus on the nature of the carriers is that they are probably large carbon-bearing molecules that reside ubiquitously in the interstellar gas (Ehrenfreund & Charnley 2000). The most promising carrier candidates are carbon chains, polycyclic aromatic hydrocarbons (PAHs), and fullerenes (Salama et al. 1996, 1999; Foing & Ehrenfreund 1994; Schulz et al. 2000; Motylewski et al. 2000). Studies on the environmental behavior of DIB carriers suggest that the strength of the DIBs results from an interplay between ionization, recombination, dehydrogenation and destruction of chemically stable, carbonaceous species (Cami et al. 1997; Sonnentrucker et al. 1997; Vuong & Foing 2000). The molecular nature of the DIB carriers is supported by the detection of substructures in the line profiles of some DIBs (Sarre et al. 1995; Ehrenfreund & Foing 1996; Krelowski & Schmidt 1997; Walker et al. 2001). Furthermore, a recent analysis of the profile of the strongest DIB ( $\lambda 4428$ ) shows a Lorentzian profile remarkably consistent with rapid internal conversion in a molecular carrier (Snow et al. 2002).

In this Letter, we present an analysis of high-resolution observations of the  $\lambda 6614$  DIB in so-called single-cloud lines of sight. The profiles show a systematic variation in the wavelengths of the observed substructure peaks. We show that these variations are most naturally explained as changes in the rotational excitation temperature in rotational contours of a large molecule. The particular band profile of this DIB also allows one to uniquely determine the rotational excitation temperature.

## 2. The $\lambda 6614$ DIB profile

The  $\lambda 6614$  DIB was first observed at high resolution by Sarre et al. (1995), revealing a clear triple-peak substructure and a red degraded wing (see Fig. 1). In a few stars, a weaker fourth and a fifth peak show up at longer wavelengths. As these are only clearly observed in two of our spectra, we will not discuss these peaks in this Letter. The substructures are intrinsic to the band profile, as the same profile shape is observed in lines of sight that only cross one interstellar cloud.

The very presence of these substructures has been explained by two different scenarios. The most popular explanation is that the profile is due to unresolved rotational contours of a large molecule, in which the three peaks represent individual branches of a rovibronic transition. Rotational contour calculations have been performed by Cossart-Magos & Leach (1990) and Kerr et al. (1996) for PAHs, by Edwards & Leach (1993) for fullerenes and by Schulz et al. (2000) for linear chains. Ehrenfreund & Foing (1996) analyzed the profiles of the  $\lambda 6614$  DIB and compared them to calculated rotational contours, concluding that the carrier of the  $\lambda 6614$  DIB has a rotational constant compatible with PAHs larger than 40 C atoms, chains of 12-18 C atoms, 30 C atom rings, or  $C_{60}$  fullerene compounds.

Alternatively, the substructures might be due to isotope shifts in large, highly symmetric molecules (Webster 1996). In this scenario, the individual peaks correspond to entities of the same molecule with a different number of  $^{13}\text{C}$  atoms. The relative intensities of the peaks then determine the abundances of the isotopic varieties (see, e.g., Walker et al. 2000).

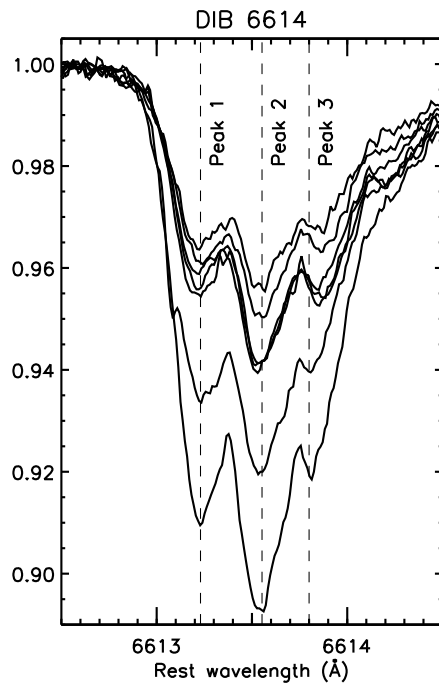


Fig. 1.— Profiles of the  $\lambda 6614$  DIB for the observed stars. All profiles are centered on the central peak (peak 2). Note how the position of the redward peak (peak 3) clearly changes from one line of sight to another. At the same time, the width of the sub peaks seems to become marginally larger. For an identification of the individual spectra, see Galazutdinov et al. (2002).

### 3. The $\lambda 6614$ DIB profile variations

Recently, Galazutdinov et al. (2002) presented new high-resolution ( $R \approx 220000$ ), high signal-to-noise ratio observations of the  $\lambda 6614$  DIB toward single-cloud lines of sight, clearly showing variability in the precise wavelengths of the peaks, and in the intensity ratios. In this Letter, we analyze those same observations; we therefore refer to Galazutdinov et al. (2002) for more observational details.

The profiles of the interstellar Na I or K I lines toward our target stars are narrow, and generally show only one main component (Galazutdinov et al. 2002), confirmed also by ultra-high resolution observations for various interstellar lines that are now available (see e.g. Welty et al. 2003, and references therein). The observed DIB profiles are therefore intrinsic.

Fig. 1 shows the profiles of the  $\lambda 6614$  DIB centered on the central peak. It is clear that there are considerable variations in the exact positions of the remaining two main peaks with respect to this central peak. The redward peak (peak 3) shows clear variations in wavelength relative to the central peak that are much larger than the individual variations in radial velocity, and therefore these variations are intrinsic. To assess the nature of these variations, we proceeded in the following way. In all proposed explanations for the substructure of the  $\lambda 6614$  DIB, the observed profile is composed of individual bands. In the rotational contour framework, these bands correspond to unresolved ro-vibronic branches; in the isotope shift scenario they correspond to different isotopomers. To accurately determine the peak positions of these individual components, we need to first decompose the profile into its components, rather than measuring the peak positions directly in the observed profile.

Galazutdinov et al. (2002) showed that nearly perfect fits to the observed line profiles can be achieved by fitting about five Gaussians to the line profiles. The three main

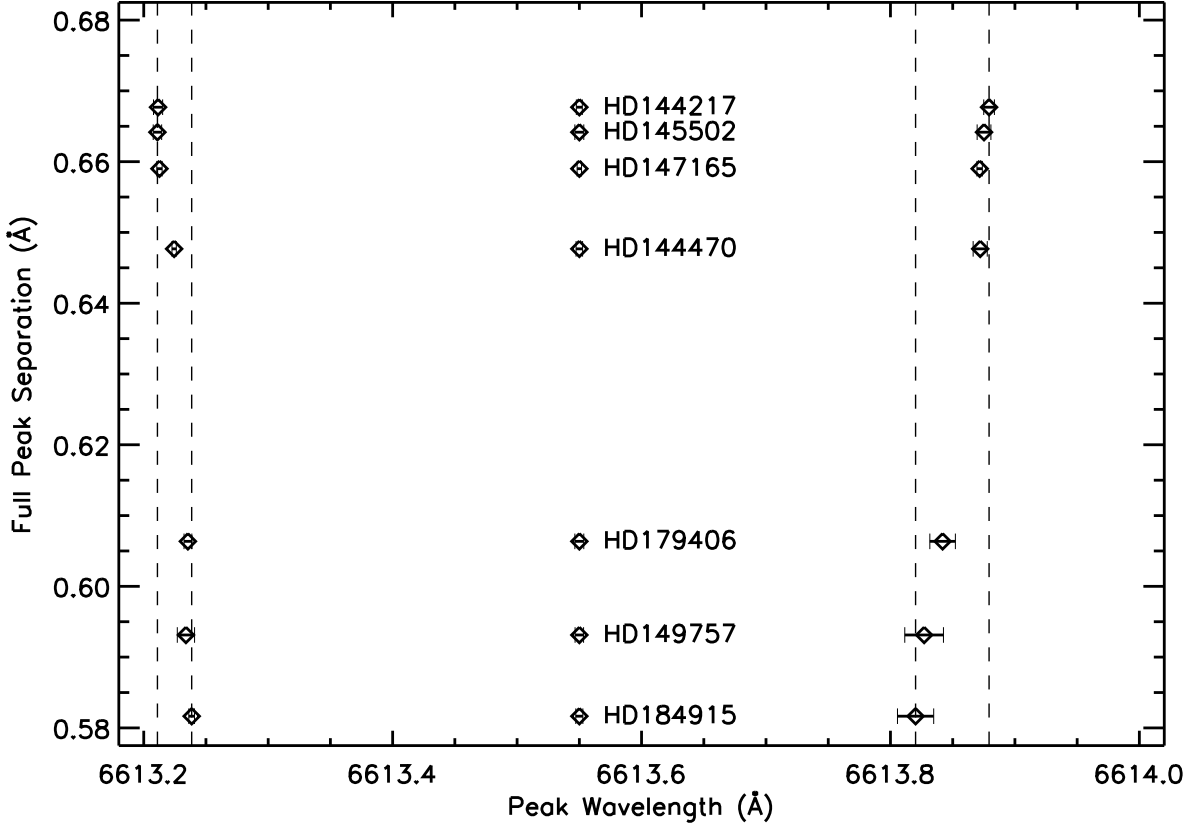


Fig. 2.— Peak positions for the three main peaks in the  $\lambda 6614$  DIB profile. Error bars are determined using a statistical approach (see text).

Gaussian components correspond to the three main peaks observed in the line profile; a fourth and fifth component are required for the additional peaks and/or the red wing. We followed a similar approach to decompose the profile into Gaussian components. The fitting routine provides a formal error estimate on the derived parameters (such as peak position) which is generally optimistic since it does not deal with systematic errors – such as the components not being true Gaussians. We therefore followed a statistical approach in which we determined the noise level on the spectra from the continuum parts outside the  $\lambda 6614$  DIB, subsequently added random noise with the same rms to the entire spectrum,

and then fitted the profile. This procedure was repeated 100 times for each spectrum, and subsequently each parameter value was taken to be the average of these 100 simulations, with the standard deviation providing a more realistic error estimate on the parameters. Using the wavelengths of the central peak (peak 2 in Fig. 1), we then shifted the individual profiles in velocity space to the same “rest” wavelength of 6613.56 Å for the central peak (Galazutdinov et al. 2000).

Fig. 2 shows the peak positions for each of the three main peaks as a function of the peak separation between the first and the third peak. The variations in the wavelengths of the sub-peaks now become much more obvious. When the redward peak (peak 3) shifts to longer wavelengths relative to the central peak, the blueward peak (peak 1) *systematically* shifts to shorter wavelengths. Whereas peak 1 shifts by about 0.03 Å (one resolution element), peak 3 shifts by twice that amount.

These variations rule out the scenario in which the substructures are due to isotope shifts; in such a case, the wavelengths of the individual peaks should be the same for each line of sight. On the other hand, the observed variations are completely consistent with the substructure being due to unresolved rotational contours and the observed variations due to changes in only one parameter : the rotational excitation temperature.

#### 4. Rotational contours

In the framework of rotational contours, the three peaks in the  $\lambda 6614$  DIB correspond to unresolved *PQR*-type branches associated with a molecular species. For any molecular species, the peak positions of these branches are determined by both molecular properties and physical parameters (such as the rotational temperature). The added value from this work – where we observe *variations* in the peak positions – stems from the fact that the



molecular properties should be the same for all lines of sight. Moreover, the triple-peak structure of the  $\lambda 6614$  DIB profile allows one to determine the molecular and physical parameters independently. This is most easily illustrated for molecules exhibiting a linear or spherical top geometry.

For linear (e.g.,  $\text{CO}_2$ ,  $\text{N}_2\text{O}$ ) or spherical top (e.g., fullerenes) geometries, the energies of the rotational levels within a vibronic band are determined by the single rotational constant  $B$  and the quantum number  $J$  (angular momentum). Selection rules on  $J$  are  $\Delta J = \pm 1$  ( $P$ - and  $R$ -branch transitions) and, in some cases (see Sect. 5),  $\Delta J = 0$  ( $Q$ -branch). For a given rotational level  $J$ , the frequencies of the  $P$  and  $R$  transitions relative to the corresponding  $Q$  transition can then be written as

$$\Delta\nu_{RQ} = 2(J+1)(B'' + \Delta B) \approx 2(J+1)B'' \quad (1)$$

$$\Delta\nu_{QP} = 2J(B'' + \Delta B) \approx 2JB'' \quad (2)$$

where  $\Delta\nu_{RQ} \equiv \nu_R - \nu_Q$  and  $\Delta\nu_{QP} \equiv \nu_Q - \nu_P$ ; the double primes refer to the lower vibronic level and  $\Delta B$  is the difference in rotational constants between the upper and lower vibronic level. Furthermore, the common approximation has been used that  $\Delta B/B'' \ll 1$ . All other things being equal, the peak absorption will arise from the most populated rotational level in the lower vibronic state. Assuming an LTE-like population distribution of the rotational levels in this lower state, it is straightforward to show that the most populated rotational level is (see e.g. Ehrenfreund & Foing 1996)

$$J_{\max} = \sqrt{\frac{kT_{\text{rot}}}{2hcB''}} - \frac{1}{2} \quad (3)$$

with  $B''$  in units of  $\text{cm}^{-1}$ . Eqs. (1), (2) and (3) nicely show how the peaks of the  $R$ - and  $P$ - branches move away from the  $Q$ -branch peak (at a different rate) when  $T_{\text{rot}}$  increases; as  $T_{\text{rot}}$  increases,  $J_{\max}$  becomes larger, and therefore both peak separations increase. This corresponds exactly to what we observe (see Fig. 2), and therefore the central peak (peak

2) in the  $\lambda 6614$  DIB must correspond to the unresolved  $Q$ -branch and peaks 1 and 3 to the  $R$ - and  $P$ -branches, respectively.

The triple-peak structure of the  $\lambda 6614$  DIB profile offers 14 independent measurements ( $\Delta\nu_{RQ}$  and  $\Delta\nu_{QP}$  for seven lines of sight) for eight free parameters ( $B''$  and seven rotational temperatures), so that all parameters can be uniquely determined. Although it is possible to determine  $B''$  and  $T_{\text{rot}}$  independently for each line of sight by manipulating Eqs. (1)–(3), the uncertainties on the derived parameters are large. Instead, we performed a  $\chi^2$  minimization to determine the eight parameters that provide the best fit to the 14 observed peak separations and determined the  $1\sigma$  uncertainties on these parameters. The best-fit parameters are listed in Table 1 and yield a reduced  $\chi^2$ -value of 1.45, indicating a good, but not a perfect fit. The derived rotational constant ( $0.016 \pm 0.003 \text{ cm}^{-1}$ ) is compatible with published values for linear and aromatic molecules, e.g.,  $\text{C}_9$  ( $0.014 \text{ cm}^{-1}$ ; van Orden et al. 1993),  $\text{HC}_7\text{N}^+$  ( $0.018 \text{ cm}^{-1}$ ; Sinclair et al. 2000),  $\text{C}_{13}\text{H}_9\text{N}$  or  $\text{C}_{15}\text{H}_9\text{N}$  ( $0.018 \text{ cm}^{-1}$ ; Mattioda et al. 2003).

For the more general case of symmetric rotors (we will not discuss the case of asymmetric rotors), the rotational energies will depend on all three rotational constants  $A$ ,  $B$ , and  $C$  (where by convention  $A \geq B \geq C$ ) and on the quantum number  $K$ , the component of the angular momentum  $J$  parallel to the symmetry axis of the molecule. The constant  $K$  can have values  $-J, -J+1, \dots, J-1, J$  so that each  $J$  level is now split up into  $2J+1$  levels with different  $K$ -values. For prolate geometries (where  $B = C$ ), these levels differ in energy by  $(A - B)K^2$ ; for oblate cases (where  $A = B$ , e.g.  $\text{C}_6\text{H}_6$ ) they differ by  $-(A - C)K^2$ . Additional selection rules are  $\Delta K = 0$  (“parallel” transitions) or  $\Delta K = \pm 1$  (“perpendicular” transitions). The observed profile will now be the superposition of all  $PQR$ -branches arising from different  $K$ -values.

For parallel transitions from the  $K = 0$  level, the additional energy term vanishes,

Table 1. The Observed Peak Separations in the  $\lambda 6614$  DIB and Derived  $T_{\text{rot}}$ -Values

Star	$\Delta\nu_{12}$	$\Delta\nu_{23}$	$\Delta\nu_{13}$	$T_{\text{rot}}$	$T_{\text{H}_2}$ <sup>a</sup>
	( $\text{cm}^{-1}$ )	( $\text{cm}^{-1}$ )	( $\text{cm}^{-1}$ )	K	K
HD 144217	0.774	0.753	1.527	$25.5^{+6}_{-4}$	88
HD 145502	0.775	0.743	1.518	$25.3^{+6}_{-4}$	90
HD 147165	0.771	0.735	1.507	$24.9^{+6}_{-4}$	64
HD 144470	0.744	0.736	1.481	$23.6^{+6}_{-4}$	73
HD 179406	0.719	0.667	1.386	$21.5^{+5}_{-4}$	—
HD 149757	0.723	0.633	1.356	$21.2^{+5}_{-4}$	54
HD 184915	0.712	0.618	1.330	$21.0^{+5}_{-3}$	69

Note. —  $B'' = 16.4 \pm 3.1 \cdot 10^{-3} \text{ cm}^{-1}$ . Quoted Uncertainties are  $1\sigma$ .

<sup>a</sup>From Savage et al. (1977). For HD 179406,  $T_{\text{H}_2}$  is unknown from observations.

and therefore Eqs. (1) and (2) still yield the correct peak separations. For parallel transitions from  $K \neq 0$ , the frequencies of the transitions will change by  $(\Delta A - \Delta B)K^2$  or  $(\Delta A - \Delta C)K^2$  compared to the  $K = 0$  frequencies. These shifts are generally small, and therefore the overall shape of the profile in terms of peak positions will not change much. In such a case, the estimates of the rotational constant  $B$  and the rotational temperature  $T_{\text{rot}}$  derived from the linear or spherical top case will still be good estimates.

For perpendicular bands, the situation is more complex. For each  $K$ , there are now two sets of  $PQR$ -branches. Compared to the linear or spherical top case, the transitions in the first set shift to the blue and in the second to the red by an amount of typically  $2(A - B)K$  for prolate tops or  $2(A - C)K$  for oblate tops. The superposition of all these branches now leads to a broadening of the observed branches, most noticeable in the  $Q$ -branch. Moreover, the  $P$ - and  $R$ -branches for oblate tops will move away from the  $Q$ -branch by  $\sim 2J_{\text{max}}(A - C)$ ; those for prolate tops move closer to the  $Q$ -branch by  $\sim 2J_{\text{max}}(A - B)$ . When using the formalism for linear or spherical top geometries to determine  $T_{\text{rot}}$ , we will therefore generally overestimate  $T_{\text{rot}}$  for oblate geometries and underestimate  $T_{\text{rot}}$  for prolate geometries.

## 5. Discussion

The observed variations in the peak positions of the substructures in the  $\lambda 6614$  DIB can be explained at least qualitatively in the rotational contour framework where the variations are due to changes in the rotational excitation temperature. The formalism for linear or spherical top geometries furthermore yields convenient expressions to uniquely determine  $B''$  and  $T_{\text{rot}}$  from the observed peak separations. Crucial in this formalism is that the central peak in the observed  $\lambda 6614$  DIB line profile is the  $Q$ -branch. However, linear and spherical top molecules only exhibit  $Q$ -branches for very specific vibronic transitions.

In those cases, the  $Q$ -branch is generally much narrower than the  $P$ - and  $R$ -branches and in many cases also much stronger. The  $\lambda 6614$  DIB, on the other hand, shows a central peak that has by and large the same width as the  $P$ - and  $R$ -branches, and a comparable strength. It seems therefore unlikely that the  $\lambda 6614$  DIB carrier conforms to a linear or spherical top geometry. Rather, the broadening of the  $Q$ -branch is presumably due to the superposition of the various stacks in a prolate or oblate top molecule. As discussed in Sect. 4, this means the values for  $T_{\text{rot}}$  in Table 1 are either too low (prolate) or too high (oblate). It is interesting to note in this context that the detailed rotational contour calculations by Kerr et al. (1996) for planar oblate tops (where  $B = 2C$ ) do indeed reproduce the width and strength of the observed subpeaks in the  $\lambda 6614$  DIB profile. Such detailed model calculations to compare to the  $\lambda 6614$  DIB variations are in progress and will be presented in a future paper. However, for the value of  $B''$  we derived, the rotational temperatures from Kerr et al. (1996) do indeed indicate slightly lower values than those in Table 1.

It is therefore tempting to conclude that the rotational temperatures for the  $\lambda 6614$  DIB carrier are indeed relatively low and, as indicated in Table 1, significantly lower than the kinetic gas temperature in the same lines of sight. This is somewhat surprising, as it has been argued that the rotational excitation temperature should actually be higher than the gas temperature (see e.g. Rouan et al. 1992; Mallocci et al. 2003). Clearly, either the rotational excitation processes (rocket effect, intramolecular vibration-rotation energy transfer, ...) included in those calculations are less important than assumed or the relaxation processes are more efficient. However, these calculations are generally carried out for large ( $\sim 100$  C atoms) PAH-like molecules. Smaller molecules or molecules of a different geometry might show a different excitation and relaxation balance. The rotational constant we derive here is indeed indicative of smaller molecules.

## 6. Conclusions

We have analyzed high-resolution and high signal-to-noise ratio spectra of the  $\lambda 6614$  DIB toward single-cloud lines of sight. The spectra clearly show a systematic shift in the relative peak position of the subpeaks, shown here for the first time. This cannot be understood if the substructure is due to isotope shifts. On the other hand, this effect can be explained both qualitatively and quantitatively by rotational contours in which only the rotational excitation temperature changes. The rotational excitation temperatures are likely to be lower than the kinetic gas temperature, indicating that for this particular DIB carrier, rotational excitation is not very efficient.

We would like to thank Bernard Foing and Xander Tielens for stimulating discussions, and the anonymous referee for making valuable suggestions. J. C. gratefully acknowledges the support of the National Research Council's Research Associateship Program. This work is supported by the NASA APRA Program (RTOP 188-01-03-01). J. K. is grateful to the Polish State Committee for Scientific Research for support under grant 2 P03D 019 23. G. G is grateful to KOSFT for providing an opportunity to work at the Korea Astronomy Observatory through the Brain Pool program and acknowledges the Ministry of Science and Technology, Korea, for support under grant M1-022-00-0005 and the Russian Foundation for Basic Research for financial support under grant 02-02-17423.

## REFERENCES

- Cami J., Sonnentrucker P., Ehrenfreund P., Foing B.H., 1997, *A&A* 326, 822
- Cossart-Magos C., Leach S., 1990, *A&A* 233, 559
- Edwards S.A., Leach S., 1993, *A&A* 272, 533
- Ehrenfreund P., Charnley S.B., 2000, *ARA&A* 38, 427
- Ehrenfreund P., Foing B.H., 1996, *A&A* 307, L25
- Foing B.H., Ehrenfreund P., 1994, *Nat* 369, 296
- Galazutdinov G., Moutou C., Musaev F., Krelowski J., 2002, *A&A* 384, 215
- Galazutdinov G.A., Musaev F.A., Krelowski J., Walker G.A.H., 2000, *PASP* 112, 648
- Herbig G.H., 1995, *ARA&A* 33, 19
- Kerr T.H., Hibbins R.E., Miles J.R., et al., 1996, *MNRAS* 283, L105
- Krelowski J., 2003, In: *Solid State Astrochemistry*, p. 147
- Krelowski J., Schmidt M., 1997, *ApJ* 477, 209
- Mallocci G., Mulas G., Benvenuti P., 2003, *A&A* 410, 623
- Mattioda A.L., Hudgins D.M., Bauschlicher C.W., Rosi M., Allamandola L.J., 2003, *J. Phys. Chem.* 107, 1486
- Motylewski T., Linnartz H., Vaizert O., et al., 2000, *ApJ* 531, 312
- Rouan D., Leger A., Omont A., Giard M., 1992, *A&A* 253, 498
- Salama F., Bakes E.L.O., Allamandola L.J., Tielens A.G.G.M., 1996, *ApJ* 458, 621

- Salama F., Galazutdinov G.A., Krełowski J., Allamandola L.J., Musaev F.A., 1999, *ApJ* 526, 265
- Sarre P.J., Miles J.R., Kerr T.H., et al., 1995, *MNRAS* 277, L41
- Savage B.D., Drake J.F., Budich W., Bohlin R.C., 1977, *ApJ* 216, 291
- Schulz S.A., King J.E., Glinski R.J., 2000, *MNRAS* 312, 769
- Sinclair W.E., Pfluger D., Verdes D., Maier J.P., 2000, *J. Chem. Phys.* 112, 8899
- Snow T.P., Zukowski D., Massey P., 2002, *ApJ* 578, 877
- Sonnentrucker P., Cami J., Ehrenfreund P., Foing B.H., 1997, *A&A* 327, 1215
- van Orden A., Hwang H.J., Kuo E.W., Saykally R.J., 1993, *J. Chem. Phys.* 98, 6678
- Vuong M.H., Foing B.H., 2000, *A&A* 363, L5
- Walker G.A.H., Bohlender D.A., Krełowski J., 2000, *ApJ* 530, 362
- Walker G.A.H., Webster A.S., Bohlender D.A., Krełowski J., 2001, *ApJ* 561, 272
- Webster A., 1996, *MNRAS* 282, 1372
- Welty D.E., Hobbs L.M., Morton D.C., 2003, *ApJS* 147, 61